Magnetic order and multipoles in the 5d2 rhenium double perovskite Ba2 Y Re O6

Gøran J. Nilsen, Corey M. Thompson, Casey Marjerisson, Danis I. Badrtdinov, Alexander A. Tsirlin, and John E. Greedan

Published version information

Citation: GJ Nilsen et al. "Magnetic order and multipoles in the 5d2 rhenium double perovskite Ba2 Y Re O6." Phys Rev B 103, no. 10 (2021): 104430.

DOI: 10.1103/PhysRevB.103.104430

Magnetic order and multipoles in the $5d^2$ rhenium double perovskite Ba_2YReO_6

Gøran J. Nilsen,[1,*] Corey M. Thompson,[2,3] Casey Marjerisson,[2] Danis I. Badrtdinov,[4] Alexander A. Tsirlin,[4,5] and John E. Greedan[2,†]

[1]*ISIS Neutron and Muon Facility, Rutherford Appleton Laboratory, Didcot OX11 0QX, United Kingdom*
[2]*Department of Chemistry, McMaster University, Hamilton, Ontario L8S 4M1, Canada*
[3]*Department of Chemistry, Purdue University, 560 Oval Drive, West Lafayette, Indiana 47907, USA*
[4]*Theoretical Physics and Applied Mathematics Department, Ural Federal University, 620002 Yekaterinburg, Russia*
[5]*Experimental Physics VI, Center for Electronic Correlations and Magnetism, Institute of Physics, University of Augsburg, 86135 Augsburg, Germany*

(Received 7 December 2020; accepted 22 February 2021; published 19 March 2021)

Ba_2YReO_6 is a double perovskite material where the Re^{5+} (d^2) ions occupy a frustrated face-centered cubic lattice. Despite strong antiferromagnetic interactions between the Re ions, as indicated by a large negative Weiss constant $\theta = -616$ K, spin freezing in Ba_2YReO_6 only occurs at 45 K. Since no long-range order of magnetic dipoles has previously been found in either muon spin rotation or neutron diffraction experiments below this temperature, it has been assumed that the low-temperature state is a spin glass. In stark contrast with these findings, we here show that Ba_2YReO_6 does in fact order with a strongly reduced dipole moment $\mu_0 = 0.29$–$0.42\ \mu_B$ via a polarized neutron diffraction experiment on a powder sample. Using the symmetries of the two likeliest magnetic structures and the properties of the $5d^2$ configuration in the presence of strong spin-orbit coupling and strong crystal fields, we use a recently derived single-ion wave function for Re^{5+} to predict a large quadrupolar moment based on the experimental μ_o.

DOI: 10.1103/PhysRevB.103.104430

I. INTRODUCTION

Magnetic order in condensed matter is usually thought of in terms of axial magnetic dipole moments that arise from unpaired electron spins. When the spin-orbit coupling and crystal field are both significant, however, entanglement between the spin and orbital angular momenta can give rise to robust and strongly interacting higher-rank multipolar degrees of freedom [1] that can produce "hidden orders"—so called because they are invisible to all but a few experimental probes. These multipolar ordered states have been widely explored in $4f$- and $5f$-electron magnetic compounds [2], most famously in URu_2Si_2 [3], as well as in $3d$ systems like V_2O_3 and Fe_2O_3 [4,5], but have only recently come to widespread attention in $5d$-electron systems [6–8]. In this particular case, the spin-orbit term in the single-ion Hamiltonian is of a similar order of magnitude to both the Hund's and crystal-field terms [9–11], and a range of behaviors can be realized depending on the balance between these and the magnetic exchange. This richness is demonstrated by the phase diagram deduced from a mean-field analysis of the geometrically frustrated face-centered cubic (FCC) lattice with two d electrons on each site [12], where the spin-orbit coupled $J = 2$ single-ion ground state can produce seven distinct dipolar and multipolar ordered phases with respect to the further neighbor ferromagnetic exchange and spin-orbit coupling strengths. Several candidate materials for multipolar order in $5d$ systems with this magnetic lattice have been identified in the double perovskite family $A_2BB'O_6$. Among these, cubic Ba_2CaOsO_6 ($Fm\bar{3}m$, Os^{6+}, d^2) has attracted particular recent attention [6,7], as it displays an ordering transition at $T = 49$ K, but no apparent dipolar magnetic order in neutron diffraction measurements. Instead, a recent theoretical study has suggested that the primary order parameter is octupolar and hence that the low-temperature phase corresponds to ferro-octupolar order [7,13].

A closely related material to Ba_2CaOsO_6 is Ba_2YReO_6 (Re^{5+}, d^2) [14,15]; the two are not only isoelectronic and isostructural but also have lattice constants that match within 0.01%. Given these similarities, the magnetic properties of Ba_2CaOsO_6 and Ba_2YReO_6 are surprisingly different, with the Weiss constant from high-temperature susceptibility indicating considerably stronger antiferromagnetic couplings in Ba_2YReO_6 ($\theta = -616$ K) than in Ba_2CaOsO_6 ($\theta = -156$ K) [15]. These differences extend to the low-temperature magnetic properties; whereas Ba_2CaOsO_6 only undergoes a single magnetic transition, Ba_2YReO_6 presents two, as evidenced by broad peaks in the specific heat at $T_u = 45$ K and $T_l = 20$ K [14]. However, both materials share an apparent absence of magnetic Bragg intensity in neutron diffraction [6,14,15], which naturally leads to the question whether Ba_2YReO_6 also supports magnetic multipoles.

In this paper, we present an experimental study of the low-temperature state in Ba_2YReO_6; polarized neutron diffraction at 1.8 K reveals the presence of several magnetic Bragg peaks that may all be indexed by an antiferromagnetic

*goran.nilsen@stfc.ac.uk
†greedan@mcmaster.ca

propagation vector $\boldsymbol{k} = (001)$. Within the mean-field phase diagram proposed in Ref. [12], the observed peaks are compatible with two experimentally indistinguishable magnetic structures: a noncollinear double-k structure and a collinear single-k structure. Fits to both models using several approximations of the Re^{5+} form factor, as well as density functional theory calculations, yield an ordered moment between $\mu_o = 0.26\ \mu_B$ and $0.42\ \mu_B$. Combining this with a symmetry-adapted wave function for Re^{5+} in the strong spin-orbit coupling limit, we find a large chargelike quadrupolar and a smaller, but still significant, magnetic octupolar moment.

II. EXPERIMENTAL

A 10 g sample of Ba_2YReO_6 was prepared as described previously and characterized by x-ray diffraction and SQUID magnetometry [14,15]. The unit cell constants and bulk magnetic properties agree well with those in the literature. For the polarized neutron diffraction experiments on the D7 instrument (Institut Laue-Langevin, France), the sample was wrapped in thin (<1 mm) strips of aluminium foil to reduce beam absorption by Re (absorption cross section $\sigma_{\text{abs}} =$ 89.7 barns). The incident wavelength of the neutron beam was $\lambda = 3.12$ Å, resulting in wave-vector moduli κ [16] for elastic scattering ranging between about 0.4 to 3.85 Å^{-1}. The transmission of the sample in this configuration was 90%.

XYZ neutron polarization analysis, where the sample scattering is measured for both polarization states of the neutron beam in three orthogonal magnetic field directions [17,18], was used to separate the weak magnetic scattering in Ba_2YReO_6 from the other components of the cross section. The six experimental cross sections were first corrected for detector efficiency and instrument polarization using measurements of vanadium and quartz, respectively. Then, the cross-section separation was performed using the established method for a wide-angle planar detector [17]. The average of the magnetic cross sections isolated from the non-spin-flip and spin-flip channels, $(d\sigma/d\Omega)_{\text{mag}}$ was used for the subsequent analysis. Data were collected at 1.8 K and 100 K, above and below the apparent spin freezing temperatures for Ba_2YReO_6. The analysis was carried out using the FULLPROF [19] and ISODISTORT [20] packages.

III. DIPOLAR MAGNETIC ORDER

The magnetic, coherent and isotope incoherent, and spin incoherent cross section components extracted from the method described above are shown in Fig. 1. At 100 K, the magnetic component shows a broad maximum around $\kappa = 0.75$ Å^{-1}, as well as several anomalies in the κ range 1.2–1.6 Å^{-1}. While the former is likely due to magnetic diffuse scattering, the latter are spurious features related to systematic errors in the polarization correction at the nuclear Bragg positions. An investigation of the spin incoherent cross section shows anomalies at the same positions in κ, confirming them as spurious.

When the temperature is reduced to 1.8 K, two sharper peaks are observed at $\kappa = 0.749(4)$ Å^{-1} and 1.055(5) Å^{-1}, alongside some persisting magnetic diffuse scattering. The

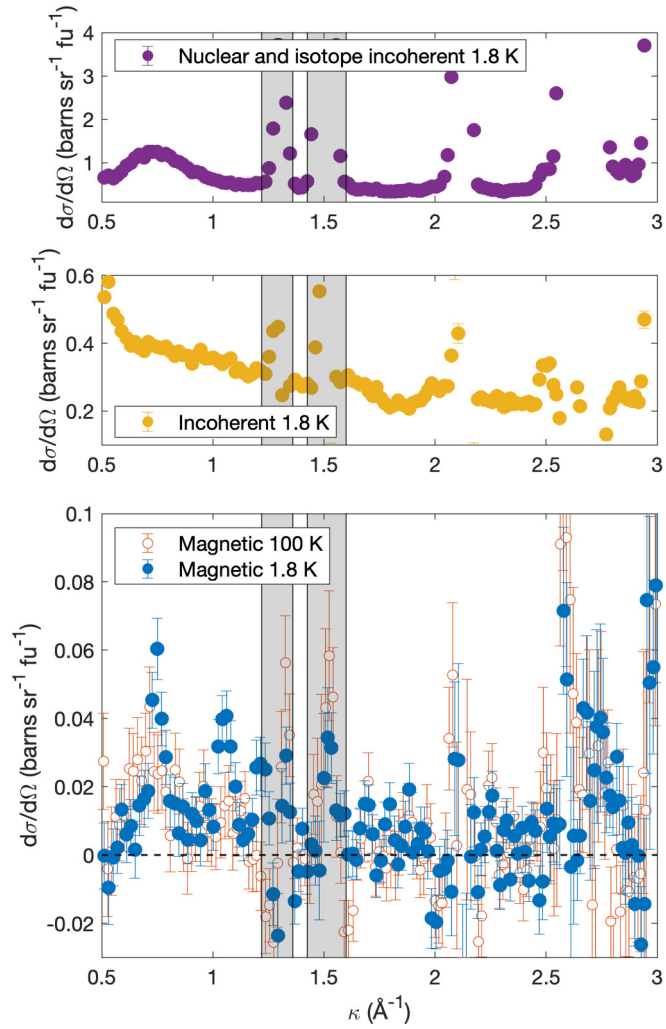

FIG. 1. Nuclear (top), spin incoherent (middle), and magnetic (bottom) neutron scattering cross sections for Ba_2YReO_6. The data in the top two panels were taken at 1.8 K. The magnetic cross section exhibits anomalies in the shaded regions near nuclear Bragg positions. At 100 K, the magnetic scattering only shows a broad feature in the vicinity of 0.75 Å^{-1}. The 1.8 K magnetic data (blue), on the other hand, show sharp features at $\kappa = 0.749(4)$ Å^{-1} and 1.055(5) Å^{-1}.

small magnitude of the peaks relative to the other cross section components— the ratio of the former to the latter is only ∼0.03—explains why these could not be seen in previous unpolarized neutron diffraction measurements. Both of the observed peaks may be indexed by the antiferromagnetic propagation vector $\boldsymbol{k} = (001)$, corresponding to the X point in the Brillouin zone of the FCC lattice. The peaks at $\kappa =$ 0.749 Å^{-1} and 1.055 Å^{-1} are then (001) and (110), respectively. This propagation vector has also been seen in numerous other magnetic double perovskite compounds, where it has typically been associated with so-called Type I order [21–24], for which collinear ferromagnetic planes of spins stack antiferromagnetically along the direction of $\boldsymbol{k}$ [Fig. 2(b)]. Type I order is typically associated with ferromagnetic next-nearest neighbor exchange.

As a starting point for our analysis, we therefore use the mean-field phase diagram derived by Chen and Balents (CB)

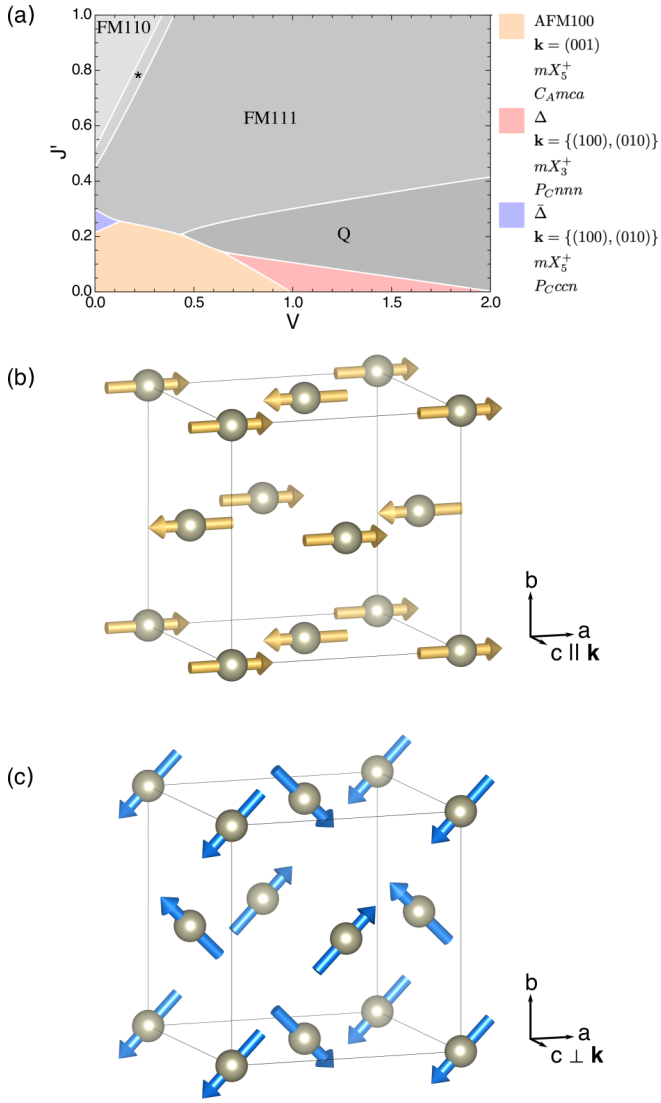

FIG. 2. (a) Mean-field magnetic phase diagram with respect to the ferromagnetic next-nearest-neighbor exchange and quadrupolar coupling for the d^2 face-centered cubic antiferromagnet with strong spin-orbit coupling, adapted from Ref. [12]. The phases relevant to the analysis in the text are highlighted in color, with details of the magnetic symmetry provided in the legend. (b), (c) Magnetic structures of the collinear AFM100 (so-called Type I) state (b) and of the $\bar{\Delta}$ state (c).

with respect to such a ferromagnetic next-nearest-neighbor exchange J' and quadrupolar coupling V for d^2 ions on a FCC lattice [12]. This is reproduced in Fig. 2, along with additional information regarding the magnetic symmetries and magnetic structures that is not given explicitly in the original paper. The seven possible states correspond to three ferromagnetic dipolar states (FM111, FM110, $*$) with fixed moment directions, three antiferromagnetic dipolar states (AFM100, Δ and $\bar{\Delta}$), and one antiferroquadrupolar state. All of the magnetic dipolar ordered states also have an underlying quadrupolar order, which either leaves the unit cell unchanged (AFM100, FM111, and $\bar{\Delta}$) or doubles it (FM110, $*$, and Δ). The octupolar order follows the dipolar order if octupolar interactions are not considered.

The absence of a bulk magnetization in measurements of Ba_2YReO_6 below T_l, combined with the presence of antiferromagnetic Bragg peaks, eliminates all three ferromagnetic orders listed above, as well as pure quadrupolar order. Three candidate states then remain: the Type-I collinear order, dubbed AFM100 by Chen and Balents, which occupies a large region of the phase diagram at small J' and V, and two smaller pockets of noncollinear order at $1 < V < 2$ and $0.2 < J' < 0.3$: the Δ and Δ' states, respectively. These three belong to the mX_5^+ (in Miller-Love notation, $\bar{\Delta}$ and AFM100) and mX_3^+ (Δ) irreducible representations (irreps) of the paramagnetic space group $Fd\bar{3}m1'$. Since the mX_3^+ irrep is incompatible with magnetic intensity at the (110) position, the Δ state is excluded. The magnetic space group for the remaining collinear AFM100 state is orthorhombic C_Amca (64.480, BNS notation), while that of the coplanar $\bar{\Delta}$ state is P_Cccn (56.375), and involves two arms of the star of $\boldsymbol{k} = \{(100), (001)\}$. The spin arrangements for both structures are depicted in Figs. 2(b) and 2(c).

IV. FORM FACTOR AND ORDERED MOMENT

Before the AFM100 and $\bar{\Delta}$ models can be compared with the experimental data, a choice must be made for the Re^{5+} form factor $f(\kappa)$, which describes the contribution of the radial part of the wave function to the magnetic scattering [25]. We begin by estimating this using $f(\kappa) = \langle j_0(\kappa)\rangle + c_2\langle j_2(\kappa)\rangle$, where $c_2 = (2-g)/g$ is obtained using either the experimentally determined Landé factor $g = 0.87$ from the high-temperature magnetic susceptibility [15] (assuming a $J = 2$ spin-orbit coupled single-ion state), $g = 2/3$ ($J = 2$, theoretical), or $g = 2$ (spin-only $S = 1$, theoretical). The latter two represent the extrema of the possible free-ion form factors given that resonant inelastic x-ray scattering has shown the spin-orbit coupling λ is similar in magnitude to the Hund's coupling J_H [10,11]. The fits are shown along with the associated $f(\kappa)$ in Fig. 3. The corresponding ordered dipole moments, which are identical for the AFM100 and $\bar{\Delta}$ [26] structures, fall in the range $\mu_o = 0.26(2)$–$0.31(2)\ \mu_B$. The ordered moment is therefore in all cases strongly reduced from the nominal $gS = 1.45\ \mu_B$ or $gJ = 1.74\ \mu_B$ (using the experimental g) for the spin-only and spin-orbit coupled cases, respectively.

The reduction in the ordered moment can arise from several different mechanisms. The first possibility is magnetic frustration; in the spin-only double perovskite Sr_2MnWO_6, for example, the ordered moment $2.27\ \mu_B$ is much smaller than $gS = 5\ \mu_B$ [27]. The moderate ratio $\theta/T_N = -14$ indicates that frustration also plays a role in Ba_2YReO_6. On the other hand, the known strong spin-orbit coupling [10] should lead to the formation of multipolar moments. Since magnetic neutron diffraction is only sensitive to odd-rank multipoles when the ground state is derived from a single J manifold, as is the case here, the quadrupolar (even-rank) component of the multipolar moment is invisible to our experiments. Furthermore, the contribution to the form factor from the octupolar moment $f(\kappa)_3 \sim \langle j_2(\kappa)\rangle - (10/3)\langle j_4(\kappa)\rangle$ is peaked at $\kappa \sim 5.5\ \text{Å}^{-1}$, well beyond the experimentally accessible κ. We will return to the possibility of multipolar moments later. Third, some of the shortfall could be the result of assuming a free-ion form

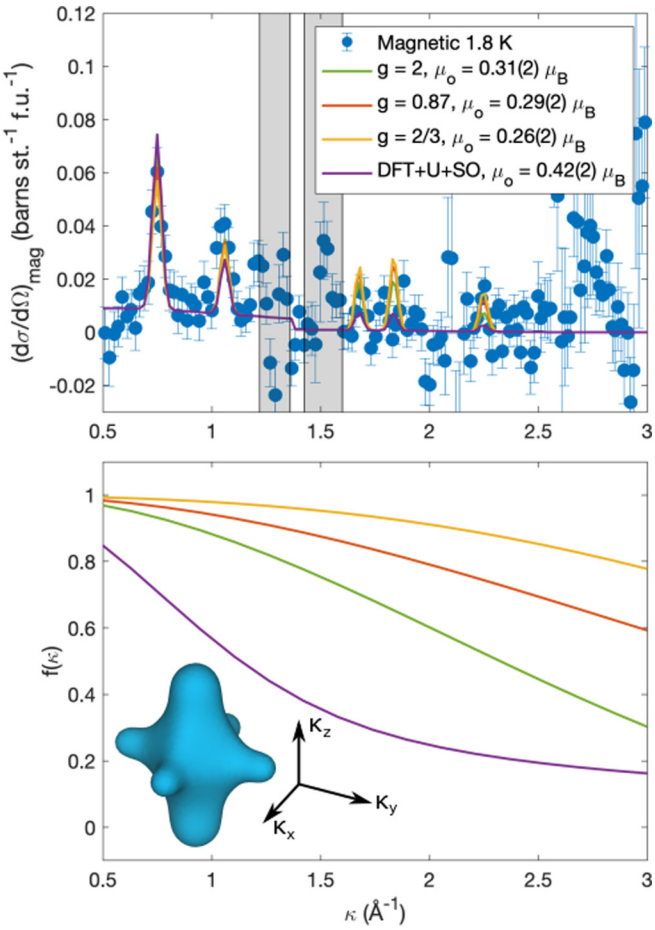

FIG. 3. Magnetic neutron scattering cross section for Ba_2YReO_6 with fits to models described in the text (solid lines). The corresponding form factors are plotted in the lower panel. The form factor isosurface from DFT + U + SO is shown for $f^2(\kappa) = 0.1$ on the bottom left.

factor, which is insufficient to describe $5d$ ions with extended d orbitals and strong covalency [28]. This is illustrated by the example of K_2IrCl_6, where the space group and Wyckoff site of the magnetic Ir^{4+} (d^4) ions are the same as in Ba_2YReO_6, and which shows drastic (up to 50%) departures from the dipolar approximation even at $\kappa \sim 1$ Å^{-1} [29]. We attempt to account for these effects by calculating the $\langle j_0(\kappa)\rangle$ contribution to the dipolar form factor by Fourier transforming the moment density obtained by density functional theory [30]; see also [31–38]. The delocalization of spin density onto the O^{2-} surrounding the Re^{5+} leads to a sharper drop in $f(\kappa)$ with increasing κ than in the free-ion case. Fitting results in a slightly higher χ^2 (1.29 versus 1.14 for $g = 2$) and $\mu_o = 0.42\ \mu_B$ (Fig. 3), still significantly lower than the moment from magnetic susceptibility.

V. MULTIPOLES AND MULTIPOLAR ORDER

Having thus placed bounds on the range of possible ordered moments in Ba_2YReO_6, we return to the implications on the possible underlying multipolar order. From a recent atomic theory [39], the dipole magnetic moment is $\mu_o = (2/3)\sin(2\chi)\ \mu_B$ where χ is the mixing angle for nonmagnetic and magnetic components of the ground state. The observed dipolar ordered moments $\mu_o = 0.26$–$0.42\ \mu_B$ are thus consistent with $\chi = 11.4°$–$19.5°$ in the absence of interactions. This implies that the chargelike quadrupole $\sim[3\cos^2(\chi) - 1]\ \mu_B$ should be large, while the magnetic octupoles $\sim\mu_o\ \mu_B$ are smaller but still significant. Although neither quadrupoles nor octupoles can be observed in the present experiment, resonant x-ray diffraction should be sensitive to both. The underlying order expected to be uncovered in such an experiment is ferroquadrupolar, although an alternate scenario of antiferroquadrupolar order has also been proposed [40]. We note that a single-crystal resonant x-ray diffraction experiment on the $5d^1$ double perovskite Ba_2MgReO_6 has revealed complex quadrupolar order at 33 K and canted antiferromagnetic order at 18 K [8]. Interestingly, this material was also thought to have a partially disordered low-temperature state.

This brings us back to the finite-temperature predictions of the mean-field Chen-Balents theory for the $5d^2$ case, which identifies three possible sequences of phase transitions into the ground state (Figs. 2 and 4 in Ref. [12]): for a quadrupolar $V > 0.3$ and next-nearest neighbor ferromagnetic $J' < 0.2$, a two-step transition to the AF100 ground state involving an intermediate antiferroquadrupolar and antiferromagnetic (Δ) state is anticipated. Indeed, two transitions (at $T_u = 45$ K and $T_l = 20$ K) are observed in Ba_2YReO_6, but previous muon spin rotation (μSR) indicates a large drop in the initial asymmetry below the upper of these, implying a static dipolar component. More surprisingly, no change in the relaxation behavior is observed at the second transition. This implies that the dipolar field at the muon site changes smoothly across the transition, despite the large changes in both the dipolar and quadrupolar orders. Also, no oscillations characteristic of dipolar long-range order are observed, in contrast with Ba_2MgReO_6, where these are paradoxically present despite the absence of magnetic Bragg intensity in neutron diffraction. The lack of oscillations in μSR could be related to static disorder or persisting dynamical fluctuations, both of which may also be the origin of the diffuse magnetic scattering observed in our polarized neutron diffraction.

VI. CONCLUSION

Ba_2YReO_6 has been studied with polarized neutron diffraction using the XYZ method [17,18]. The ground state of Ba_2YReO_6 can now be assigned as ordered, erasing the ambiguity of earlier studies. The dipolar component of this order is probably either the collinear (AFM100/Type-I, C_Amca) or noncollinear ($\bar{\Delta}$, P_Cccn) antiferromagnetic structures proposed in Ref. [12]. The ordered dipolar moment falls in the range 0.26–0.42 μ_B depending on the choice of magnetic form factor and is therefore strongly reduced versus the expected Re^{5+} moment. The implications of this can be understood by considering a recently derived local Re^{5+} wave-function based on the symmetry of the low-temperature phase, which indicates a large quadrupolar moment, and hence underlying quadrupolar order. The same may be the case for other $5d^2$ systems with reduced ordered moments, like Ba_2LuReO_6 [24]. Despite the finding of magnetic order in Ba_2YReO_6, the persistence of diffuse scattering in the ordered phase indicates a fluctuating or disordered component that can

explain the absence of oscillations in previous μSR studies. The results are in general strikingly different to Ba_2CaOsO_6, where no magnetic intensity was seen at the (001) position in temperature-subtracted data [6], but muon oscillations are observed. A deeper understanding of both the single-ion magnetism in Ba_2YReO_6 and Ba_2CaOsO_6 and their multipolar orders can be realized once single crystals become available.

ACKNOWLEDGMENTS

We thank A. A. Aczel, D. D. Khalyavin, and S. W. Lovesey for useful discussions, and S. W. Lovesey for several useful comments on the paper. J.E.G. thanks the Natural Sciences and Engineering Research Council (NSERC) of Canada for support through the Discovery Grant Program.

[1] M.-T. Suzuki, H. Ikeda, and P. M. Oppeneer, First-principles theory of magnetic multipoles in condensed matter systems, J. Phys. Soc. Jpn. **87**, 041008 (2018).

[2] P. Santini, S. Carretta, G. Amoretti, R. Caciuffo, N. Magnani, and G. H. Lander, Multipolar interactions in f-electron systems: The paradigm of actinide dioxides, Rev. Mod. Phys. **81**, 807 (2009).

[3] J. A. Mydosh and P. M. Oppeneer, Colloquium: Hidden order, superconductivity, and magnetism: The unsolved case of URu_2Si_2, Rev. Mod. Phys. **83**, 1301 (2011).

[4] S. W. Lovesey and K. S. Knight, Resonant x-ray Bragg diffraction from orbital moments in vanadium sesquioxide (V_2O_3) and haematite (α-Fe_2O_3), J. Phys.: Condens. Matter **12**, L367 (2000).

[5] A. Rodríguez-Fernández, J. A. Blanco, S. W. Lovesey, V. Scagnoli, U. Staub, H. C. Walker, D. K. Shukla, and J. Strempfer, Chiral properties of hematite α-Fe_2O_3 inferred from resonant Bragg diffraction using circularly polarized x rays, Phys. Rev. B **88**, 094437 (2013).

[6] D. D. Maharaj, G. Sala, M. B. Stone, E. Kermarrec, C. Ritter, F. Fauth, C. A. Marjerrison, J. E. Greedan, A. Paramekanti, and B. D. Gaulin, Octupolar versus Néel Order in Cubic $5d^2$ Double Perovskites, Phys. Rev. Lett. **124**, 087206 (2020).

[7] S. Voleti, D. D. Maharaj, B. D. Gaulin, G. Luke, and A. Paramekanti, Multipolar magnetism in d-orbital systems: Crystal field levels, octupolar order, and orbital loop currents, Phys. Rev. B **101**, 155118 (2020).

[8] D. Hirai, H. Sagayama, S. Gao, H. Ohsumi, G. Chen, T.-h. Arima, and Z. Hiroi, Detection of multipolar orders in the spin-orbit-coupled $5d$ Mott insulator Ba_2MgReO_6, Phys. Rev. Res. **2**, 022063(R) (2020).

[9] W. Witczak-Krempa, G. Chen, Y. B. Kim, and L. Balents, Correlated quantum phenomena in the strong spin-orbit regime, Annu. Rev. Condens. Matter Phys. **5**, 57 (2014).

[10] B. Yuan, J. P. Clancy, A. M. Cook, C. M. Thompson, J. Greedan, G. Cao, B. C. Jeon, T. W. Noh, M. H. Upton, D. Casa, T. Gog, A. Paramekanti, and Y.-J. Kim, Determination of Hund's coupling in $5d$ oxides using resonant inelastic x-ray scattering, Phys. Rev. B **95**, 235114 (2017).

[11] A. Paramekanti, D. J. Singh, B. Yuan, D. Casa, A. Said, Y.-J. Kim, and A. D. Christianson, Spin-orbit coupled systems in the atomic limit: Rhenates, osmates, iridates, Phys. Rev. B **97**, 235119 (2018).

[12] G. Chen and L. Balents, Spin-orbit coupling in d^2 ordered double perovskites, Phys. Rev. B **84**, 094420 (2011).

[13] S. W. Lovesey and D. D. Khalyavin, Lone octupole and bulk magnetism in osmate $5d^2$ double perovskites, Phys. Rev. B **102**, 064407 (2020).

[14] T. Aharen, J. E. Greedan, C. A. Bridges, A. A. Aczel, J. Rodriguez, G. MacDougall, G. M. Luke, V. K. Michaelis, S. Kroeker, C. R. Wiebe, H. Zhou, and L. M. D. Cranswick, Structure and magnetic properties of the $S = 1$ geometrically frustrated double perovskites La_2LiReO_6 and Ba_2YReO_6, Phys. Rev. B **81**, 064436 (2010).

[15] C. M. Thompson, J. P. Carlo, R. Flacau, T. Aharen, I. A. Leahy, J. R. Pollichemi, T. J. S. Munsie, T. Medina, G. M. Luke, J. Munevar, S. Cheung, T. Goko, Y. J. Uemura, and J. E. Greedan, Long-range magnetic order in the $5d^2$ double perovskite Ba_2CaOsO_6: Comparison with spin-disordered Ba_2YReO_6, J. Phys.: Condens. Matter **26**, 306003 (2014).

[16] We use κ in preference to $|Q|$ for consistency with Ref. [39] .

[17] O. Schärpf and H. Capellmann, The xyz-difference method with polarized neutrons and the separation of coherent, spin incoherent, and magnetic scattering cross sections in a multidetector, Phys. Status Solidi (a) **135**, 359 (1993).

[18] J. R. Stewart, P. P. Deen, K. H. Andersen, H. Schober, J.-F. Barthélémy, J. M. Hillier, A. P. Murani, T. Hayes, and B. Lindenau, Disordered materials studied using neutron polarization analysis on the multi-detector spectrometer, D7, J. Appl. Cryst. **42**, 69 (2009).

[19] J. Rodríguez-Carvajal, Recent advances in magnetic structure determination by neutron powder diffraction, Phys. B: Condens. Matter **192**, 55 (1993).

[20] B. J. Campbell, H. T. Stokes, D. E. Tanner, and D. M. Hatch, *ISODISPLACE*: A web-based tool for exploring structural distortions, J. Appl. Cryst. **39**, 607 (2006).

[21] P. Battle, J. Goodenough, and R. Price, The crystal structures and magnetic properties of Ba_2LaRuO_6 and Ca_2LaRuO_6, J. Solid State Chem. **46**, 234 (1983).

[22] A. E. Taylor, R. Morrow, D. J. Singh, S. Calder, M. D. Lumsden, P. M. Woodward, and A. D. Christianson, Magnetic order and electronic structure of the $5d^3$ double perovskite Sr_2ScOsO_6, Phys. Rev. B **91**, 100406(R) (2015).

[23] S. Vasala and M. Karppinen, $A_2B'B''O_6$ perovskites: A review, Prog. Solid State Chem. **43**, 1 (2015).

[24] J. Xiong, J. Yan, A. A. Aczel, and P. M. Woodward, Type I antiferromagnetic order in Ba_2LuReO_6: Exploring the role of structural distortions in double perovskites containing $5d^2$ ions, J. Solid State Chem. **258**, 762 (2018).

[25] K. Kobayashi, T. Nagao, and M. Ito, Radial integrals for the magnetic form factor of 5d transition elements, Acta Cryst. A **67**, 473 (2011).

[26] The angle of the spins in the ab plane cannot be determined because the sum of the intensities contributing to each observed reflection is independent of it. C_Amca and P_Cccn cannot be distinguished for the same reason.

[27] A. Azad, S. Ivanov, S.-G. Eriksson, H. Rundlöf, J. Eriksen, R. Mathieu, and P. Svedlindh, Structural and magnetic properties of the double perovskite Sr_2MnWO_6, J. Magn. Magn. Mater. **237**, 124 (2001).

[28] L. Xu, N. A. Bogdanov, A. Princep, P. Fulde, J. van den Brink, and L. Hozoi, Covalency and vibronic couplings make a nonmagnetic j = 3/2 ion magnetic, npj Quantum Mater. **1**, 16029 (2016).

[29] J. W. Lynn, G. Shirane, and M. Blume, Covalency Effects in the Magnetic form Factor of Ir in K_2IrCl_6, Phys. Rev. Lett. **37**, 154 (1976).

[30] See Supplemental Material at http://link.aps.org/supplemental/10.1103/PhysRevB.103.104430 for more information about the DFT and DFT+U+SO calculations that were used to determine the Re^{5+} form factor.

[31] P. Giannozzi, S. Baroni, N. Bonini, M. Calandra, R. Car, C. Cavazzoni, D. Ceresoli, G. L. Chiarotti, M. Cococcioni, I. Dabo *et al.*, QUANTUM ESPRESSO: A modular and open-source software project for quantum simulations of materials, J. Phys.: Condens. Matter **21**, 395502 (2009).

[32] G. Pizzi, V. Vitale, R. Arita, S. Blügel, F. Freimuth, G. Géranton, M. Gibertini, D. Gresch, C. Johnson, T. Koretsune *et al.*, Wannier90 as a community code: New features and applications, J. Phys.: Condens. Matter **32**, 165902 (2020).

[33] D. I. Badrtdinov, V. V. Mazurenko, and A. A. Tsirlin, Origin of up-up-down-down magnetic order in Cu_2GeO_4, Phys. Rev. B **100**, 214401 (2019).

[34] N. Marzari and D. Vanderbilt, Maximally localized generalized Wannier functions for composite energy bands, Phys. Rev. B **56**, 12847 (1997).

[35] K. Koepernik and H. Eschrig, Full-potential nonorthogonal local-orbital minimum-basis band-structure scheme, Phys. Rev. B **59**, 1743 (1999).

[36] V. V. Mazurenko, I. V. Solovyev, and A. A. Tsirlin, Covalency effects reflected in the magnetic form factor of low-dimensional cuprates, Phys. Rev. B **92**, 245113 (2015).

[37] J. Hembacher, D. I. Badrtdinov, L. Ding, Z. Sobczak, C. Ritter, V. V. Mazurenko, and A. A. Tsirlin, Stripe order and magnetic anisotropy in the $S = 1$ antiferromagnet $BaMoP_2O_8$, Phys. Rev. B **98**, 094406 (2018).

[38] J. P. Perdew, K. Burke, and M. Ernzerhof, Generalized Gradient Approximation Made Simple, Phys. Rev. Lett. **77**, 3865 (1996).

[39] S. W. Lovesey, D. D. Khalyavin, G. van der Laan, and G. J. Nilsen, Diffraction by multipoles in a $5d^2$ rhenium double perovskite, Phys. Rev. B **103**, 104429 (2021).

[40] C. Svoboda, M. Randeria, and N. Trivedi, Orbital and spin order in spin-orbit coupled d^1 and d^2 double perovskites, arXiv:1702.03199.